International Journal on Recent and Innovation Trends in Computing and Communication
ISSN: 2321-8169 Volume: 12 Issue: 2
Article Received: *25 November 2023* ***Revised:*** *12 December 2023* ***Accepted:*** *30 January 2024*

Enhanced Isolation and Performance in MIMO Antenna for 5G Applications

Saif Nadhim Galib
Department of Electrical Engineering, Faculty of Engineering
Razi University
Bagdad, Iraq
Saifalsaidy100@gmail.com

Seyed Vahab AL-Din Makki
Department of Electrical Engineering, Faculty of Engineering
Razi University
Kermanshah, Iran
v.makki@razi.ac.ir

Abstract— This paper introduces a compact multiple-input multiple-output (MIMO) antenna design tailored for 5G cellular applications. The proposed array comprises four identical, compact antenna elements designed to deliver extensive radiation coverage and support diverse functionalities. Each antenna element is based on a dual-polarized square-ring resonator, which is fed by two T-shaped feed lines and operates at a frequency of 3.7 GHz, making it suitable for the 5G frequency band. The paper highlights the significance of achieving optimal isolation between adjacent elements and presents straightforward yet effective decoupling techniques to address this. These techniques include the incorporation of sixteen zigzag slots between the radiator and feeder, a T-shaped feed line, rectangular slots within the feeders, a defected ground plane, and the strategic arrangement of radiating elements at varying orientations. The designed antenna achieves a bandwidth of 550 MHz (ranging from 3.45 to 4 GHz) and exhibits high-gain radiation patterns with minimal envelope correlation coefficient (ECC) and total active reflection coefficient (TARC). Experimental measurements validate that the antenna's performance aligns closely with the anticipated characteristics, demonstrating its reliability for practical 5G applications.

Keywords-5G; MIMO system; Dual-polarized antenna; Decoupling techniques; Defected ground structures (DGS); Resonator antenna, Smartphone

I. INTRODUCTION

Driven by advantages such as very high speeds, lower latency, and outstanding reliability, the ongoing advancement of mobile communication technology has prompted researchers worldwide to take a growing interest in 5G mobile communication systems [1]. Additionally, factors like increased channel capacity, excellent spectrum efficiency, and significant connection density further highlight the importance of this technology [2]. In 5G terminals, antennas are designed to be highly efficient with a low profile, wide operational bandwidth, and excellent mutual coupling properties, particularly for hand-held devices [3]. Microstrip antennas are ideal for cellular applications due to their cost-effectiveness and ease of integration, making them especially advantageous given the limited space available on smartphone boards [4]. Compact microstrip-fed printed antennas are particularly promising for smartphones due to their flat design, simple structure, and ease of integration with RF circuits, which help overcome the limitations on antenna size imposed by smartphone boards [5].

Recently, several designs for smartphone antennas targeting 5G applications have been proposed, focusing mainly on frequency ranges below 6 GHz [6]. However, many of these designs use single-polarized resonators, which occupy significant space on the non-planar mainboard structure, leading to restricted and poor radiation coverage. An innovative eight-port, four-element antenna design offers extensive radiation coverage and compact radiators [7]. Zigzag slots are used to enhance radiation efficiency and broaden the frequency range, but they may increase the likelihood of signal loss if not precisely fabricated. The T-shaped feed line improves power distribution but can complicate achieving proper matching between the feeder and the radiator. Rectangular slots enhance power flow but may lead to unwanted reflections. The defected ground plane reduces interference but can cause uneven power distribution and undesirable reflections if not carefully designed. Arranging radiating elements at different angles enhances directivity but can make controlling the radiation pattern more challenging.

In comparison to these methods, this research introduces an innovative approach that integrates all these techniques—slots between the radiator and feeder, a T-shaped feed line, rectangular slots within the feeder, a defected ground plane, and the strategic arrangement of radiating elements at varying orientations. By combining these techniques, a multi-layered defense against mutual coupling is created, with each technique addressing different aspects of electromagnetic interaction between antenna elements. This integrated approach results in a more comprehensive reduction in mutual coupling than any single method could achieve alone, clearly distinguishing the proposed approach from conventional methods and underscoring the significance of this work in antenna design. The proposed antenna design, optimized for a frequency of 3.7 GHz within the sub-6 GHz range of the 5G spectrum, was

International Journal on Recent and Innovation Trends in Computing and Communication
ISSN: 2321-8169 Volume: 12 Issue: 2
Article Received: *25 November 2023* ***Revised:*** *12 December 2023* ***Accepted:*** *30 January 2024*

developed using the CST software suite [8]. The proposed MIMO architecture was also implemented, and its performance was rigorously evaluated through measurements [9].

To verify the accuracy of the antenna's performance, measurement data were compared with electromagnetic simulations [10]. Unlike previously developed MIMO antennas, our design offers notable characteristics such as excellent isolation, extensive radiation coverage, minimal ECC, TARC, and good signal integrity [11]. Moreover, channel capacity loss (CCL) is crucial as it directly impacts the efficiency of data transmission. The proposed design addresses this by optimizing the antenna structure to enhance channel capacity and reduce losses [12]. The following sections provide a detailed explanation of the key attributes of each radiator and the overall array design [13].

This paper is structured into four main sections. The first section provides a comprehensive introduction that outlines the importance of the research and the need for improvements in antenna design. The second section presents the research idea and applies it to a 2x2 MIMO antenna, including detailed calculations and performance analysis. In the third section, we scale up the design to an 8x8 MIMO configuration aimed at enhancing performance for 5G mobile phones, and we conduct thorough testing on this antenna to evaluate its performance. Finally, the fourth section summarizes the key findings and offers recommendations for future work.

II. SINGLE-ELEMENT ANTENNA

Figure 1 shows the suggested design schematic. A square-ring resonator is present on the top layer of the antenna configuration, accompanied by a pair of T-shape feed lines. Additionally, sixteen zigzag slots between the square ring and T-shape feed line, a square slot on the bottom layer of the antenna (DGS), and rectangular slots in the feed line to minimize the mutual coupling that could occur between the ports of the antenna. The proposed design was printed on an FR4 insulating substrate with relative loss (δ=0.025) and transmittance (ε=4.4), which is of thickness 1.6 mm.

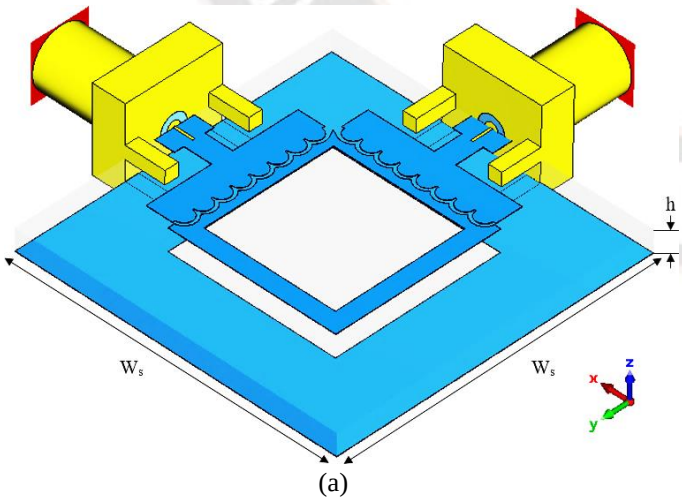

(a)

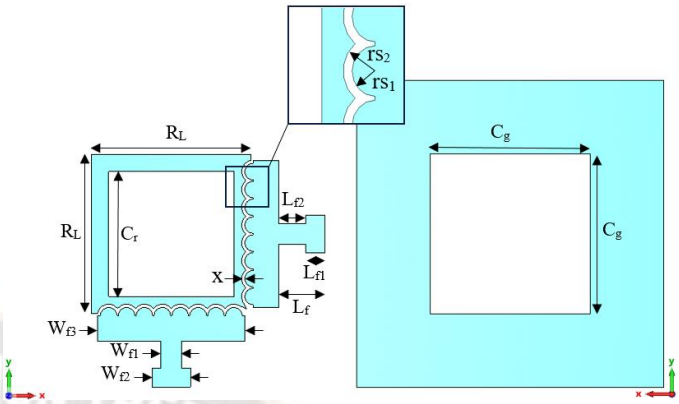

(b)

Figure 1: (a) Side-view (b) front-layer, and (c) back-layer of the proposed antenna element.

The overall figure 2 illustrates five different antenna designs, each representing a stage of antenna development. In Figure 2(a), the first design (Ant. 1) features a simple square structure fed by a T-shaped feed line, representing a basic design focused solely on the fundamental structure without additional features. The second design (Ant. 2) modifies the structure by replacing the square resonator with a square-ring resonator. The third antenna (Ant. 3) introduces a square slot in the ground plane beneath the resonator, aiming to improve current distribution and enhance performance at the required frequency. The fourth design (Ant. 4) retains the square ring while adding zigzag slots between the square ring and the T-shaped feed line, which enhances the coupling between the feed line and the resonator and reduces interference between different elements of the antenna. Finally, the fifth design (Ant. 5) combines all previous improvements with the addition of two rectangular slots in each feed line, representing the final stage of development focused on achieving the best possible performance through these subtle design refinements. These designs demonstrate a gradual evolution, with each stage introducing simple yet impactful enhancements to optimize performance. Figure 2(b) shows the S-parameters (S11 and S12) for each design stage, illustrating how each modification contributes to improved frequency response and overall performance.

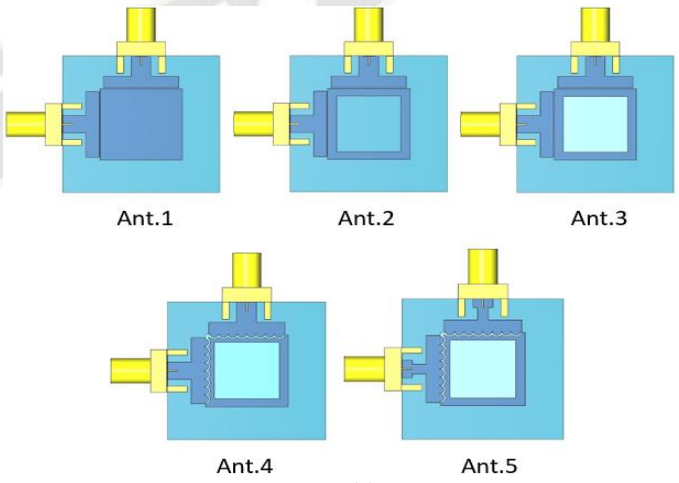

(a)

International Journal on Recent and Innovation Trends in Computing and Communication
ISSN: 2321-8169 Volume: 12 Issue: 2
Article Received: *25 November 2023* ***Revised:*** *12 December 2023* ***Accepted:*** *30 January 2024*

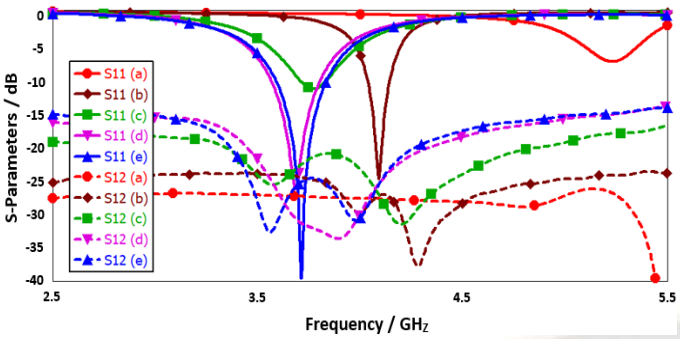

(b)

Figure 2: (a) Stages of development of the proposed antennas (a-e), and (b) S-parameter results of the antennas

Table 1: The parameter values of the proposed design.

Parameter	Value (mm)	Parameter	Value (mm)
Cr	10	W_{f1}	1.6
R_L	12.5	W_{f2}	3
X	0.25	W_{f3}	11.5
C_g	13	r_{S1}	0.65
W_S	24	rs_2	0.9
L_f	3.6	$L_{s\ MIMO}$	150
L_{f1}	1.5	$W_{s\ MIMO}$	75
L_{f2}	2.1		

performance, particularly in terms of the operating frequency range, impedance matching, and mutual coupling.

The design of the Square-ring Resonator antenna is influenced by several critical factors that significantly impact its Figure 3 provides a detailed analysis of the S-parameters (S11 and S12) of the antenna across different values of key design parameters, including the microstrip feed line length (Lf), the side length of the inner square-ring resonator (Sr), the zigzag space between the square-ring resonator and the T-shaped feed line (X), and the square slot in the ground plane (Cg). In Figure 3(a), the variations in S11 and S21 characteristics are examined for different values of Lf. It is observed that an Lf of 3.6 mm enhances the antenna's impedance bandwidth as compared with the other values. Figure 3(b) explores the effect of altering the Sr dimensions, which significantly impacts the impedance bandwidth. Figure 3(c) highlights the influence of varying the X parameter on the antenna's resonant frequency, with a value of X=0.25 mm resulting in a resonant frequency around 3.7 GHz. This indicates the critical role of this parameter in tuning the antenna. It was also observed that increasing X generally degrades impedance matching, as reflected by higher S11 values, suggesting a trade-off between frequency tuning and matching performance. Finally, Figure 3(d) presents the S-parameter performance for different values of Cg. The selected value strikes a balance between achieving optimal impedance bandwidth and maintaining sufficient isolation, with Cg=13 mm proving to be the most effective configuration. Additionally, the results show that as Cg increases, the resonant frequency shifts and impedance matching becomes less effective. After studying these parameters and selecting the optimal values, they were applied to the final antenna design to achieve the highest possible performance.

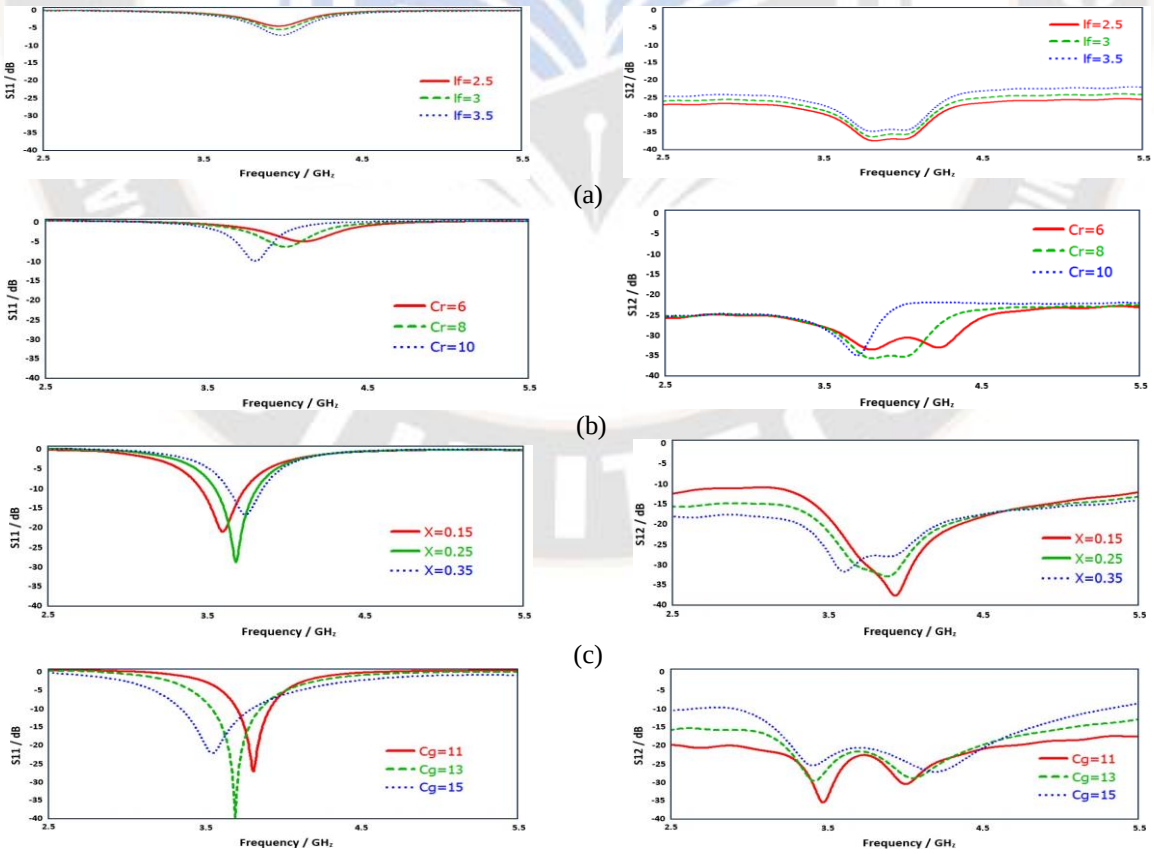

(a)

(b)

(c)

(d)

Figure 3: S11 and S21 results of the antenna for various values of (a) l_f, (b) Cr, (c) X, (d) Cg

International Journal on Recent and Innovation Trends in Computing and Communication
ISSN: 2321-8169 Volume: 12 Issue: 2
Article Received: *25 November 2023* ***Revised:*** *12 December 2023* ***Accepted:*** *30 January 2024*

Figure X presents the performance analysis of the zigzag edge square ring resonator antenna in terms of return loss. At a resonance frequency of 3.7 GHz, the antenna demonstrates a return loss (S11) of -40 dB. It covers a bandwidth of 300 MHz from 3.6 GHz to 3.9 GHz at a -10 dB return loss level, and the bandwidth extends to 550 MHz from 3.45 GHz to 4 GHz at a -6 dB return loss. Additionally, a remarkably low mutual coupling between antenna elements is observed, approximately -31 dB at the resonance frequency. This frequency selection is particularly advantageous for 5G applications due to its optimal balance between capacity and data transmission speeds.

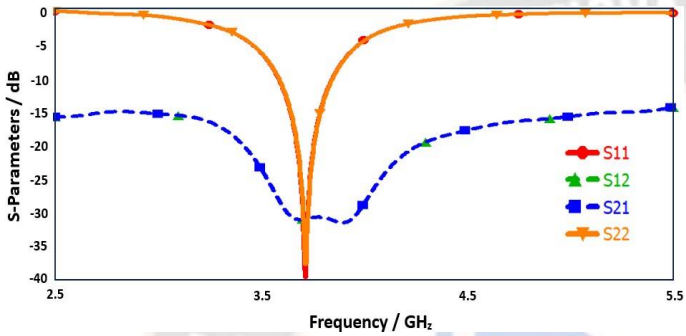

Figure 4: S-Parameter of single antenna element.

Figure 5 illustrates the surface current distribution at different feed ports of the antenna operating at 3.7 GHz. It shows that the surface currents are primarily concentrated around the square-ring resonator. Additionally, the current densities are equal and opposite, which supports the polarization diversity function of the antenna.

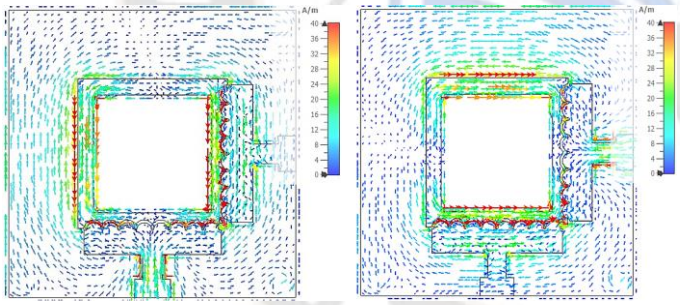

(a) (b)

Figure 5: Current distribution at 3.7 GHz for (a) port 1, and (b) port 2

The evaluation of the 3D radiation pattern is essential for depicting energy distribution, directivity, and identifying potential interference within antenna systems. This analytical process is crucial for optimizing the design of multi-antenna systems and enhancing energy efficiency. Figures 6 (a) and (b) illustrate the consistent radiation patterns of the antenna at 3.7 GHz under varied feed conditions (port 1 and port 2), each exhibiting orthogonal polarizations. The antenna achieves a gain of over 3.5 dBi. Characterized predominantly by a quasi-spherical or omnidirectional radiation pattern, it ensures uniform coverage across all directions, facilitating effective signal distribution.

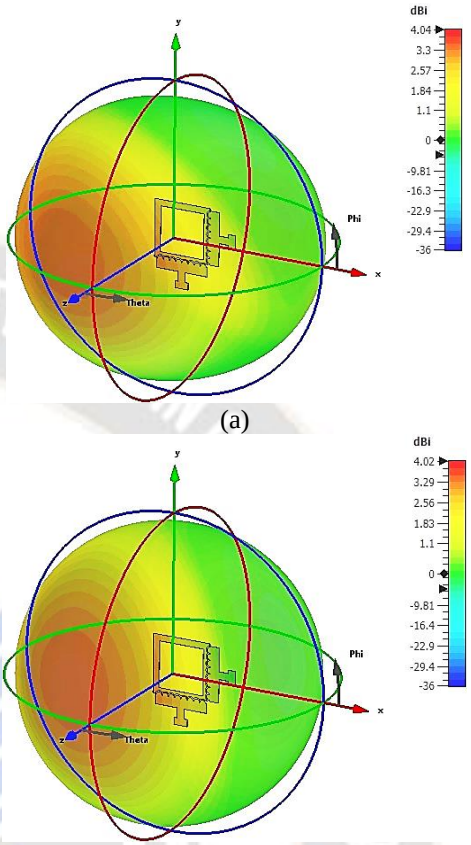

(a)

(b)

Figure 6: 3D radiation patterns of the proposed antenna at 3.7 GHz for (a) port 1 and, (b) port 2

The efficiency and maximum gain of the proposed antenna design are presented in Figure 7. The results indicate that the antenna operates with a radiation efficiency of 92% and a total efficiency of 80% across the entire frequency range. Additionally, the antenna's maximum gain ranges from 4.5 to 4.8 dBi.

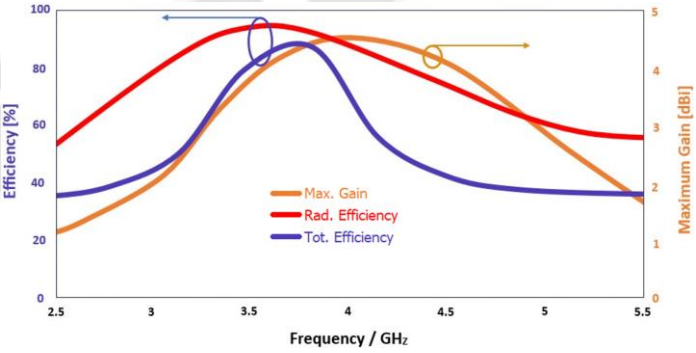

Figure 7: Efficiencies, and maximum gain for single-element antenna

The final form of the proposed antenna design is fabricated and tested as shown in figures 8 and figure 9. Figure 8 shows the photograph of the manufactured antenna. Figure 9 shows the S-

International Journal on Recent and Innovation Trends in Computing and Communication
ISSN: 2321-8169 Volume: 12 Issue: 2
Article Received: *25 November 2023* ***Revised:*** *12 December 2023* ***Accepted:*** *30 January 2024*

parameters simulation and measurement results. Based on the given results, we can tell that there is a convergence between them.

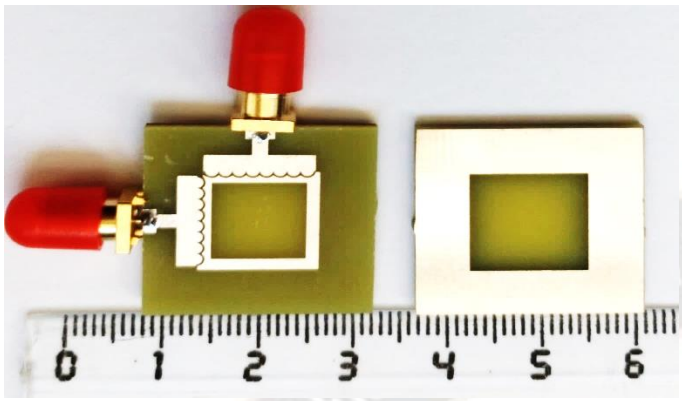

(a) (b)

Figure 8: photographs of the fabricated antenna (a) tested design, (b) top view, and bottom view.

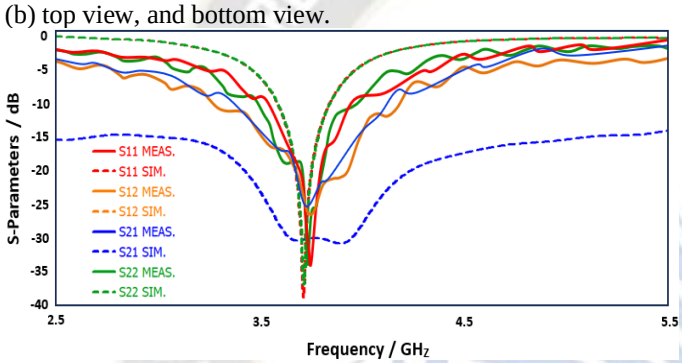

Figure 9: Simulated and Measured S-parameters for single-element antenna

III. The Proposed MIMO 5G Smartphone Antenna

The antenna shown in the image is part of an 8x8 MIMO (Multiple-Input Multiple-Output) system, specifically designed to operate at a frequency of 3.7 GHz. This frequency is highly significant in modern wireless communication applications, including 5G networks, where high data rates and reliable communications are essential. The proposed design integrates four 2x2 antennas, each strategically positioned at the corners of the PCB. Each individual antenna consists of square ring resonators with 16 zigzag edges and a slotted ground plane. Each antenna element is fed by a dual T-shaped feed line with 16 zigzag edges. The feed lines are arranged perpendicularly to achieve dual polarization, enhancing isolation and the overall performance of the antenna. The proposed antenna is designed on an FR-4 substrate with dimensions of 150 × 75 × 1.6 mm^3. Operating at a frequency of 3.7 GHz, the antenna provides a good balance between range and data transfer rate, making it suitable for environments that require handling multiple signals simultaneously.

When these four 2x2 antennas are combined into an 8x8 MIMO configuration, the system becomes capable of handling a large number of data streams simultaneously, significantly enhancing data rates and overall efficiency. Figure 10 provides a comprehensive overview of the proposed MIMO antenna design. Figure 10(a) presents a side view of the antenna, highlighting the basic parameters and port distribution. Figures 10(b) and 10(c) show the front and back views of the proposed MIMO antenna design, respectively.

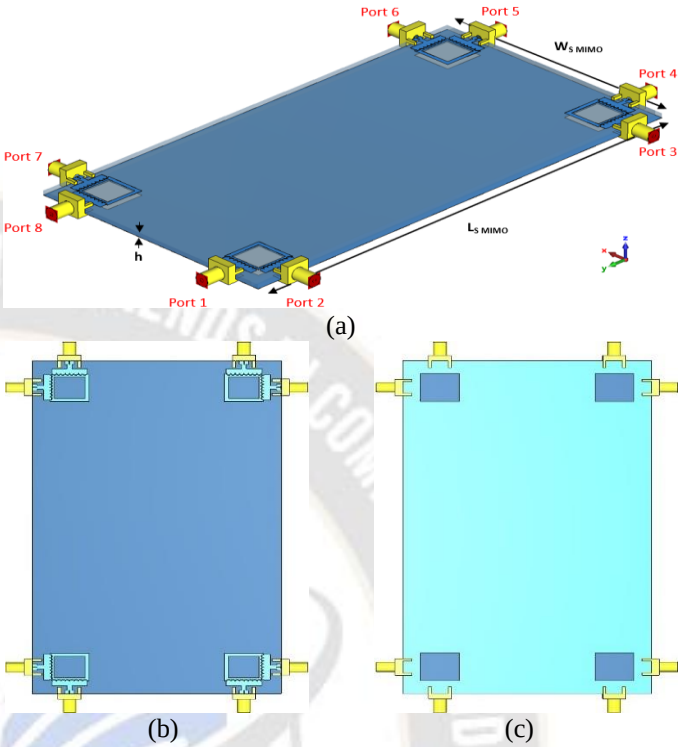

(a)

(b) (c)

Figure 10: (a) Side, (b) front, and (c) back views of the design

The radiation elements in the MIMO antenna exhibit return loss characteristics similar to those of the single-element antennas. The antenna demonstrates excellent impedance matching, with reflection coefficients around -28 dB at 3.7 GHz, as shown in Figure 11(a). Moreover, the mutual coupling between the antenna elements remains below -25 dB, as illustrated in Figure 11(b), which is sufficient to prevent any significant degradation in radiation performance. This makes the design ideal for 5G smartphone applications.

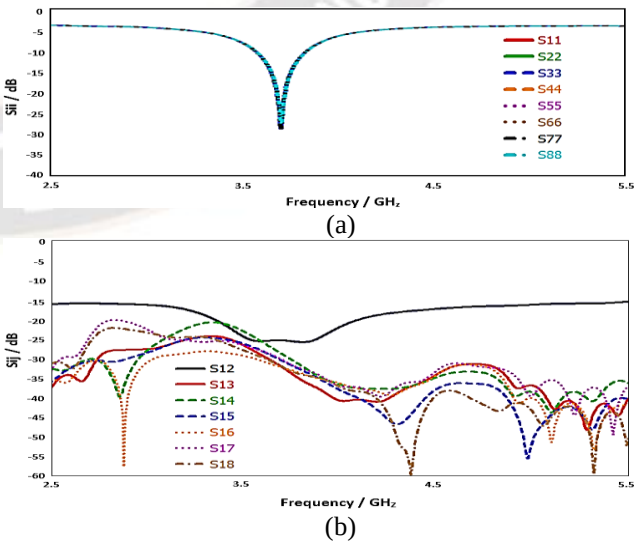

(a)

(b)

Figure 11 S-parameter results for MIMO antenna, Sii, and Sij

International Journal on Recent and Innovation Trends in Computing and Communication
ISSN: 2321-8169 Volume: 12 Issue: 2
Article Received: *25 November 2023* ***Revised:*** *12 December 2023* ***Accepted:*** *30 January 2024*

Figures 12(a) and 12(b) illustrate the envelope correlation coefficient (ECC) and the total active reflection coefficient (TARC) for the proposed design. These characteristics can be calculated from the S-parameter results using the formulas Eq. (1) and Eq. (2). The ECC remains below 0.04 across the entire bandwidth, indicating minimal correlation between adjacent elements. At 3.7 GHz, the TARC value is less than -23, demonstrating the antenna's suitability for MIMO applications [15].

$$ECC = \frac{|Sjj* Sji+Sij* Sii|^2}{(1-|Sjj|^2-|Sji|^2)(1-|Sij|^2-|Sii|^2)}\ dB \qquad (1)$$

$$TARC = \sqrt{\frac{(Sjj+Sji)^2+(Sij+Sii)^2}{2}}\ dB \qquad (2)$$

where, Sii and Sjj are the return losses, Sij and Sji are the mutual coupling.

Another critical parameter for evaluating the MIMO performance of a multi-antenna design is the channel capacity loss (CCL), which arises from the mutual correlation between antenna elements in MIMO systems. The degradation in system performance can be quantified by the capacity loss. The CCL in a MIMO system is primarily influenced by the S-parameters. For an 8 × 8 MIMO system, the CCL can be calculated using the formulas described below. It is important to note that the acceptable limit for CCL is ≤0.4 bps/Hz [11].

$$CCL = \log_2 \det(\Psi^{SNR}) \qquad bps/Hz \qquad (3)$$

where the Ψ^{SNR} is the channel SNR determined as:

$$\Psi^{SNR} = \begin{bmatrix} p_{ii} & \cdots & p_{ij} \\ \vdots & \ddots & \vdots \\ p_{ji} & \cdots & p_{jj} \end{bmatrix} \qquad (4)$$

where

$$p_{ii} = 1 - (|s_{ii}|^2 + |s_{ij}|^2)$$
$$p_{ij} = -(s_{ii} * s_{ij} + s_{ji} * s_{ij})$$

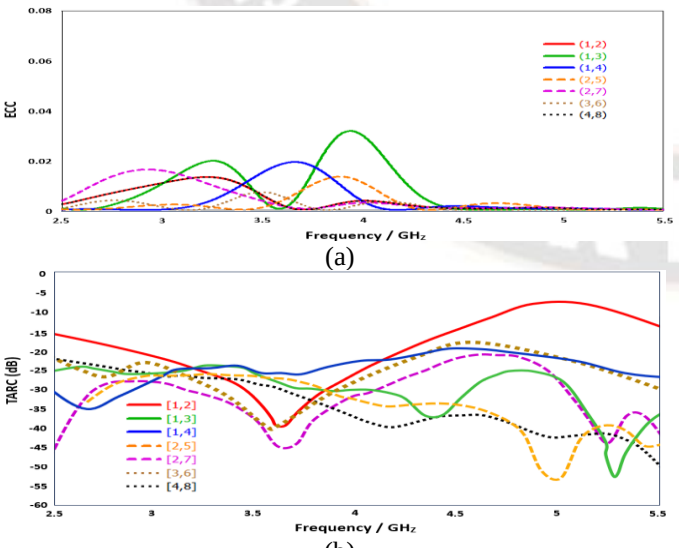

(a)

(b)

Figure 12: Simulated MIMO antenna, ECC, and TARC

As illustrated in Figure 13, the proposed MIMO design exhibits very low CCL across its entire operational band, maintaining values below 0.4 bps/Hz within the 3.45–4 GHz frequency range.

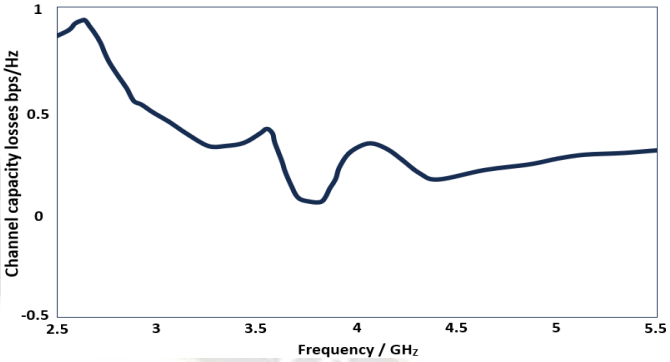

Figure 13: CCL of the Proposed MIMO antenna proposed design

The diversity gain results for the proposed MIMO antenna system over the frequency range from 2.5 to 5.5 GHz are shown in Figure 14, where the value exceeds 9.9 dB, confirming the efficiency of the proposed design. Diversity gain is one of the key metrics for evaluating the performance of MIMO systems.

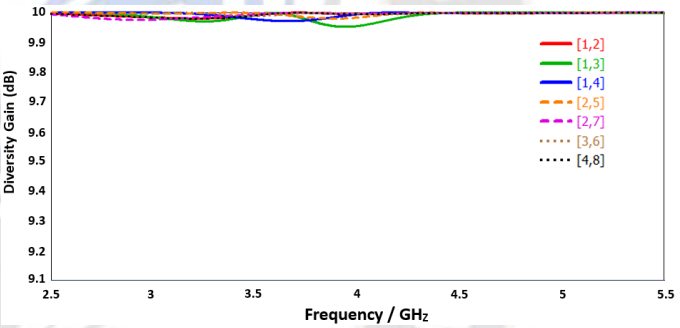

Figure 14: Diversity gain of the MIMO antenna proposed design

Figure 15 shows two types of efficiencies: radiation efficiency and total efficiency, over the frequency range from 2.5 to 5.5 GHz. The figure indicates that radiation efficiency reaches 79% at the resonant frequency of 3.7 GHz, while total efficiency peaks at 55% at the same frequency.

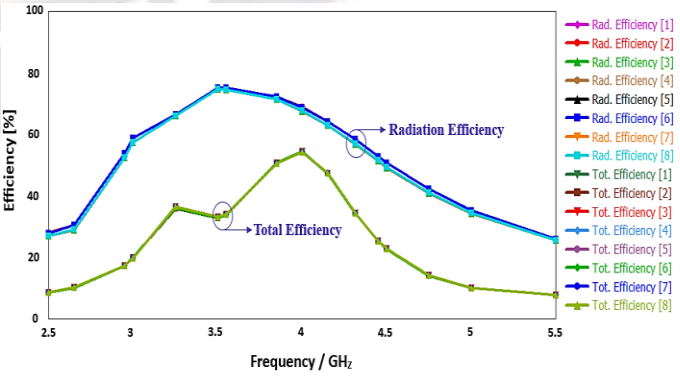

Figure 15 Efficiencies of the proposed MIMO antenna design

International Journal on Recent and Innovation Trends in Computing and Communication
ISSN: 2321-8169 Volume: 12 Issue: 2
Article Received: *25 November 2023* ***Revised:*** *12 December 2023* ***Accepted:*** *30 January 2024*

Figure 16 shows the 3D radiation patterns of each antenna element integrated into the printed circuit board (PCB) of the proposed 5G smartphone. The radiation patterns of the radiators demonstrate their ability to cover all sides of the smartphone PCB. Meanwhile, due to the dual-polarization property of the antenna elements, different polarizations can be achieved for each area of the PCB, making the MIMO antenna system suitable for mobile terminal applications. The radiation patterns of the antenna were calculated at 3.7 GHz under various feeding conditions (port 1 - port 8). The antenna achieves a gain of 5 to 7.5 dBi.

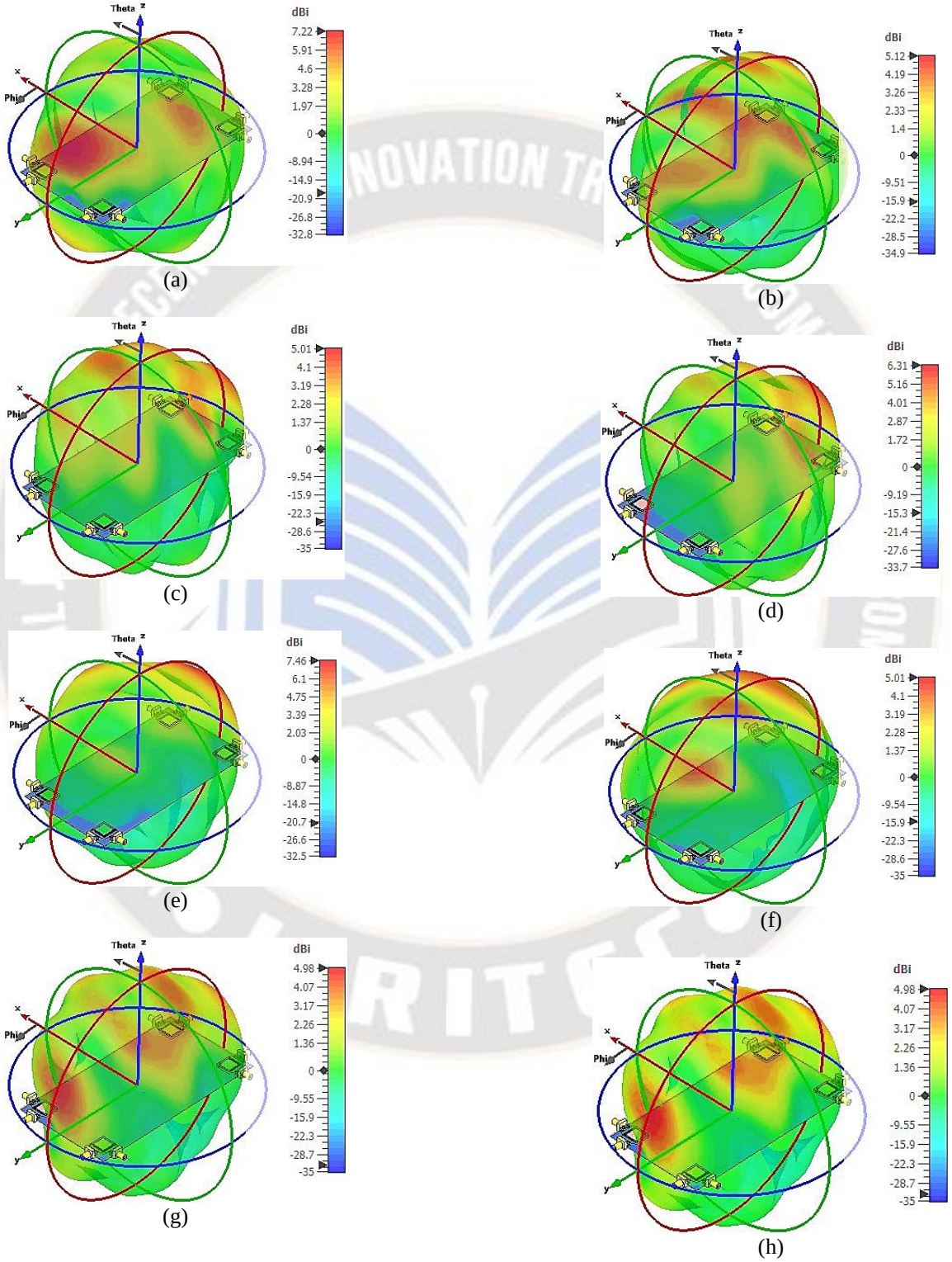

Figure 16. 3D radiation patterns for the 8 antenna elements at 3.7 GHz (a) antenna 1, (b) antenna 2, (c) antenna 3, (d) antenna 4, (a) antenna 5, (b) antenna 6, (c) antenna 7, and (d) antenna 8

International Journal on Recent and Innovation Trends in Computing and Communication
ISSN: 2321-8169 Volume: 12 Issue: 2
Article Received: *25 November 2023* ***Revised:*** *12 December 2023* ***Accepted:*** *30 January 2024*

Figure 17 illustrates the radiation patterns of the antenna elements in the proposed MIMO system when operating in Talk-mode, taking into account the user's head. The figure demonstrates that the MIMO antenna system effectively maintains sufficient gain across the radiators, which are strategically positioned at various corners of the PCB.

The gain for the antenna elements varies depending on their specific locations within the talk-mode configuration, ranging from 5 dB to 6.3 dB. The figure provides valuable insights into how the MIMO system adapts to such conditions, ensuring reliable communication with minimal signal degradation.

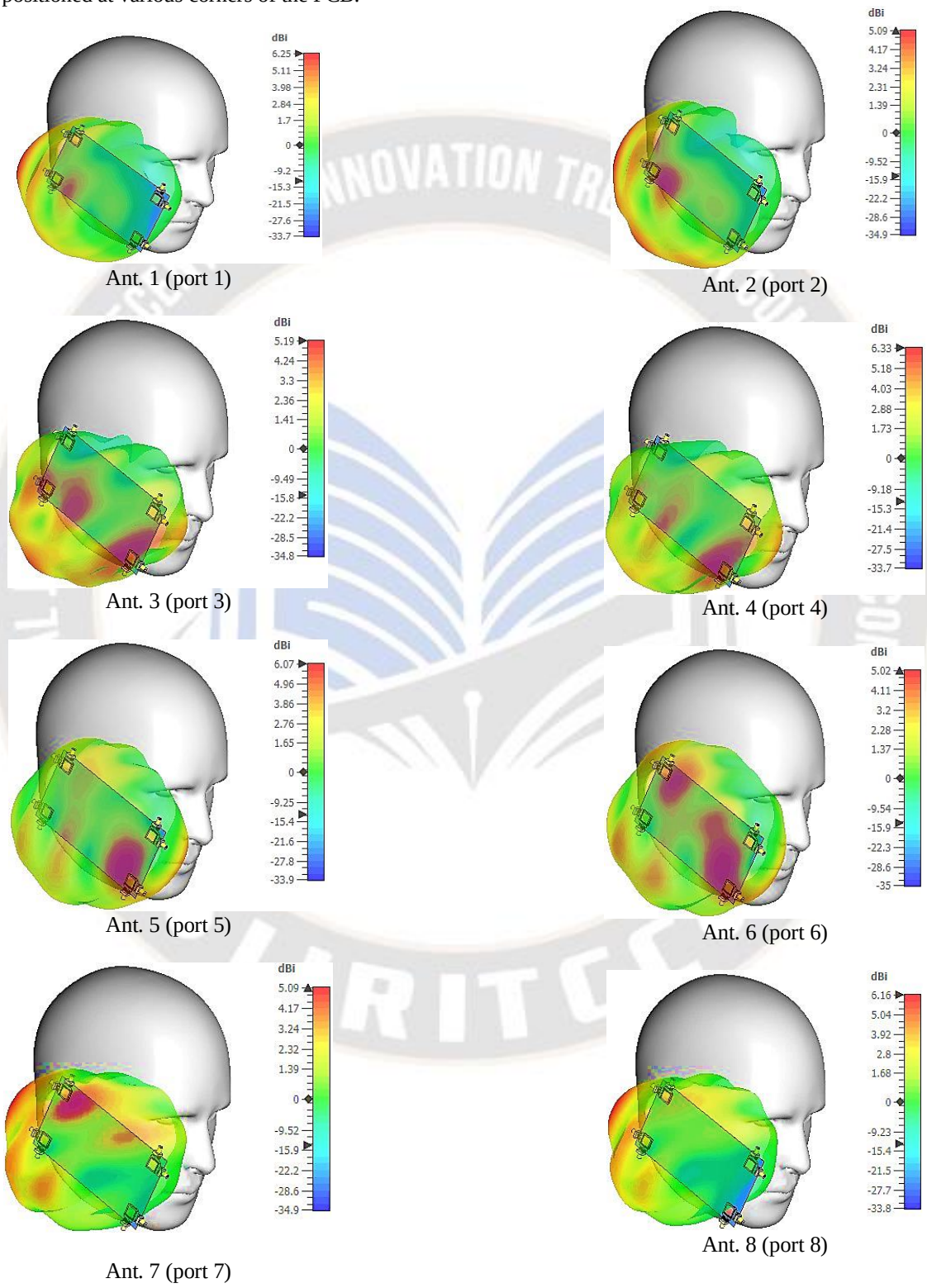

Figure 17: Radiation pattern of the antenna elements in use mode for (port1-port8)

International Journal on Recent and Innovation Trends in Computing and Communication
ISSN: 2321-8169 Volume: 12 Issue: 2
Article Received: *25 November 2023* ***Revised:*** *12 December 2023* ***Accepted:*** *30 January 2024*

Table 2 compares the proposed antenna with existing designs in terms (number of antenna elements, bandwidth, efficiency, size, isolation, ECC, and gain). The proposed antenna offers a broader bandwidth (3.45-4 GHz) and higher isolation (-25 dB), surpassing other designs. Its total efficiency (55-79%) and compact size (150x75 mm²) are competitive, ensuring suitability for 5G applications.

The antenna's extremely low ECC (<0.004) indicates excellent signal diversity, making it ideal for reducing interference and enhancing communication reliability in MIMO systems. It is important to note that many of the previous works do not address the gain. This omission limits the scope of their analysis and provides an incomplete assessment of MIMO antenna performance

Table 2: Comparisons of a proposed antenna with recently released MIMO antennas

Ref.	Antenna elements	Bandwidth (GHz)	Efficiency (%)	Size (mm^2)	Isolation (Sij) (-dB)	ECC	Gain dBi
[14]	8x8	3.4-3.8	70-80	150x75	>13	<0.01	NA
[15]	8x8	3.4-3.6 (-6dB)	45-60	124x74	>15	<0.15	4.8
[16]	8x8	3.4-3.6	62-78	140x70	>10	<0.2	7.2
[17]	8x8	3.3-5	>46	150x75	>14.5	<0.1	3.3-5
[18]	8x8	3.2-3.9	82-96	120x60	>15	<0.01	NA
[19]	8x8	3.4-3.6	43-52.5	150x75	>12	<0.13	NA
[20]	8x8	3.3-3.6 (-6dB)	44-53	100x40	>15	<0.15	2
[21]	8x8	3.4-3.6	56-66	150x75	>15	<0.02	NA
[22]	8x8	3.3-3.6 (-6dB)	42-75	155x75	>13	<0.15	NA
proposed antenna	2 x 2 & 8 x 8	3.25-3.85 3.45-4	85-95 55-79	24x24 150x75	22 25	<0.04	4-4.5 5-7.5

IIII. CONCLUSION

This manuscript presents an enhanced design for a resonator antenna aimed at optimizing 5G MIMO mobile terminals. The proposed configuration features an eight-port setup with four modified square-ring resonators positioned at the corners of the mobile phone mainboard. To minimize mutual coupling, the design incorporates sixteen zigzag slots between the radiators and feeders, a T-shaped feed line, rectangular slots within the feeders, a defected ground plane, and a strategic arrangement of radiating elements at varying orientations. The MIMO antenna design ensures comprehensive radiation coverage and supports dual polarization on both sides of the PCB, which is crucial for effective 5G communication. The antenna was fabricated and tested, revealing a strong correlation between simulated and measured results. The radiators operate within a frequency range of 3.25 to 3.85 GHz for a single antenna element and 3.45 to 4 GHz for the MIMO antenna, with a resonance at 3.7 GHz. A thorough investigation was conducted into the critical aspects of the smartphone antenna design, including S-parameters, efficiency, radiation patterns, gain, ECC, TARC, and CCL results.

ACKNOWLEDGEMENT

The research work of this article is fabricated and measured in microwave lab in Department of Electrical Engineering, Razi University, Kermanshah, Iran.

FINDING

The authors of the paper reported that there is no funding associated with the work featured in the article.

CONFLICTS OF INTEREST

The authors declare no conflict of interest.

REFERENCES:

[1] A. Ren, Y. Liu, H. Yu, Y. Jia, C. Sim, and Y. Xu, "A High Isolation Building Block Using Stable Current Nulls for 5G Smartphone Applications," *IEEE Access*, vol. 60, pp. 170419–170429, 2019.

[2] K. Ming, H. Wahl, K. Man, and C. Hou, "Circularly Polarized Patch Antenna for Future 5G Mobile Phones," *IEEE Access*, vol. 2, pp. 1521–1529, 2014.

[3] N. Parchin, J. Zhang, R. Abd-Alhameed, G. Pedersen, and S. Zhang, "A Planar Dual-Polarized Phased Array with Broadband Width and Quasi-Endfire Radiation for 5G Mobile Handsets," *IEEE Transactions on Antennas and Propagation*, vol. 69, no. 10, pp. 6410–6419, 2021.

[4] A. Ullah, N. Parchin, A. Amar, and R. Abd-Alhameed, "Phased Array Antenna Design with Improved Radiation Characteristics for Mobile Handset Applications," in Proceedings of the 16th European Conference on Antennas and Propagation (EuCAP), pp. 14, 2022.

[5] Q. Lai, Y. Pan, and S. Zheng, "A Self-Decoupling Method for MIMO Antenna Array Using Characteristic Mode of Ground Plane," *IEEE Transactions on Antennas and Propagation*, vol. 71, no. 3, pp. 2126–2135, 2023.

[6] M. Khatkar, M. Vigenesh, S. Verma, G. Premananthan, S. Sharma, and P. Mathurkar, "5G Dual Polarized Sectoral Antenna and Its Design with MIMO Channel," in *6th International Conference on Contemporary Computing and Informatics (IC3I)*, 2023.

[7] Z. Chen, T. Yuan, and H. Wong, "A Miniaturized MIMO Antenna with Dual-Band for 5G Smartphone Application," *IEEE Open Journal of Antennas and Propagation*, vol. 4, pp. 111–117, 2023.

[8] CST Microwave Studio, Version 2023, CST, Framingham, MA, USA, 2023.

[9] H. Kiani, A. Altaf, M. Anjum, S. Afridi, Z. Arain, S. Anwar, S. Khan, M. Ali Bakhshikenari, A. Lalbakhsh, M. A. Khan, R. A. Abd-Alhameed, and E. Limiti, "MIMO Antenna System for Modern 5G Handheld Devices with Healthcare and High Rate Delivery," *Sensors*, vol. 21, no. 21, pp. 119, 2021.

[10] K. Wong, C. Tsai, and J. Lu, "Two Asymmetrically Mirrored Gap-Coupled Loop Antennas as a Compact Building Block for Eight-Antenna MIMO Array in the Future Smartphone," *IEEE Transactions on Antennas and Propagation*, vol. 65, no. 4, pp. 1765–1778, 2017.

[11] S. Kiani, H. Savci, H. Abubakar, N. Parchin, H. Rimli, and B. Hakim, "Eight-Element MIMO Antenna Array with Tri-Band Response for Modern Smartphones," *IEEE Access*, vol. 11, pp. 44244–44253, 2023.

[12] S. N. Islam, M. Kumar, G. Sen, and S. Das, "Design of a Compact Triple Band Antenna with Independent Frequency Tuning for MIMO Applications," *International Journal of RF and Microwave Computer-Aided Engineering*, pp. 1–10, 2019.

[13] M. Ameen, Richa, and R. Chaudhary, "Isolation and Gain Enhancement of MIMO Diversity Antenna Using Metamaterial Absorber and Linear-to-Circular Polarization Converter," in *IEEE Microwaves, Antennas, and Propagation Conference (MAPCON)*, 2023.

[14] K. Wong, C. Tsai, and J. Lu, "Two Asymmetrically Mirrored Gap-Coupled Loop Antennas as a Compact Building Block for Eight-Antenna MIMO Array in the Future Smartphone," *IEEE Transactions on Antennas and Propagation*, vol. 65, no. 4, pp. 1765–1778, 2017.

[15] W. Jiang, B. Liu, Y. Cui, and W. Hu, "High-Isolation Eight-Element MIMO Array for 5G Smartphone Applications," *IEEE Access*, vol. 7, pp. 34104–34112, 2019.

[16]] J. Guo, L. Cui, C. Li, and B. Sun, "Side-Edge Frame Printed Eight-Port Dual-Band Antenna Array for 5G Smartphone Applications," *IEEE Transactions on Antennas and Propagation*, vol. 66, no. 12, pp. 7412–7417, 2018.

[17] A. Zhao and Z. Ren, "Wideband MIMO Antenna Systems Based on Coupled-Loop Antenna for 5G N77/N78/N79 Applications in Mobile Terminals," *IEEE Access*, vol. 7, pp. 93761–93771, 2019.

[18] Q. H. Kareem and M. J. Farhan, "Compact Dual-Polarized Eight-Element Antenna with High Isolation for 5G Mobile Terminal Applications," *International Journal of Intelligent Engineering and Systems*, vol. 14, no. 6, pp. 187–197, 2021.

[19] M. Li, Y. Ban, Z. Xu, G. Wu, C. Sim, K. Kang, and Z. Yu, "Eight-Port Orthogonally Dual-Polarized Antenna Array for 5G Smartphone Applications," *IEEE Transactions on Antennas and Propagation*, vol. 64, no. 9, pp. 3820–3830, 2016.

[20] C. F. Ding, X. Y. Zhang, C. D. Xue, and C. Y. D. Sim, "Novel Pattern-Diversity-Based Decoupling Method and Its Application to Multi-Element MIMO Antenna," *IEEE Transactions on Antennas and Propagation*, vol. 66, no. 10, pp. 4976–4985, 2018.

[21] M. Y. Muhsin, A. J. Salim, and J. K. Ali, "A Compact Self-Isolated MIMO Antenna System for 5G Mobile Terminals," *Computer Systems Science & Engineering*, vol. 42, no. 3, pp. 920–934, 2022.

[22] D. Huang, Z. Du, and Y. Wang, "Slot Antenna Array for Fifth-Generation Metal Frame Mobile Phone Applications," *International Journal of RF and Microwave Computer-Aided Engineering*, vol. 29, no. 9, pp. 1–9, 2019.